Available online at www.sciencedirect.com
ScienceDirect
Journal of Power Sources 166 (2007) 194–201
JOURNAL OF POWER SOURCES
www.elsevier.com/locate/jpowsour

Transport in packed-bed and wall-coated steam-methanol reformers

Ming-tsang Lee*, Ralph Greif, Costas P. Grigoropoulos, Hyung Gyu Park, Frank K. Hsu

Department of Mechanical Engineering, University of California at Berkeley, Berkeley, CA 94720-1740, USA

Received 30 November 2006; received in revised form 2 January 2007; accepted 3 January 2007
Available online 16 January 2007

Abstract

Methanol-steam reforming can be utilized as a fuel processing system for hydrogen fuel cells. A study of the reacting flow in packed-bed and wall-coated catalytic reactors is presented. The wall-coated reformer has a smaller power requirement for delivering fuel than the packed catalytic bed reformer. Also, the coated catalytic layer has a smaller thermal resistance compared to the packed catalytic bed. This yields enhanced thermal field management for the wall-coated reformer that is essential for reformer performance. Understanding the transport in reformers is essential for improving both the efficiency of the reforming process and the quality of the processed fuel.

Keywords: Fuel cell; Methanol conversion; Packed-bed reformer; Wall-coated reformer

1. Introduction

Increased energy demand and environmental protection considerations promote the need for improved energy conversion systems. Among these systems, fuel cells are attractive due to their low pollution, high potential efficiency and ease of recharging. Various types of fuel cells provide a variety of suitable solutions for different energy requirements. For the applications of portable electrical power, especially for personal mobile electronics, proton exchange membrane (PEM) fuel cells are considered desirable owing to their relatively low operating temperatures, small volume and light weight [1]. In particular, miniature PEM fuel cells based on micro scale design and fabrication technologies are compatible with the continuously growing areas of integrated circuits (IC) and microelectrochamical systems (MEMS) [2]. This yields the requirement for developing compatible fuel processors for converting hydrocarbons to hydrogen rich gas as a fuel for miniature fuel cells. Methanol has been considered as a suitable hydrocarbon for miniature PEM fuel cell applications because of its high volumetric and gravimetric energy densities, safe handling, ease of storage and conversion to hydrogen at low temperatures (∼250 °C) [2,3].

The design of fuel processors or reformers can correspond to small volume, small weight, low cost, long lifetime, low byproduct (carbon monoxide), ease of manufacture, low flow resistance, low thermal resistance and short start-up time [3]. Miniature or micro methanol reformers provide the potential to achieve these requirements and have attracted great interest [4]. Several micro-reformers based on MEMS technologies have been fabricated and tested [5–14]. Micro-reformers made by packing catalyst particles into micro channels have the advantage of easy catalyst loading. However, high flow resistance resulting from the packing catalyst particles may limit the design and performance of micro-reformers [15–17].

Recently, micro-reformers with wall-coated or suspended catalytic layer configurations have been studied due to their lower transport resistances compared to packed-bed reformers [5–11]. In the present work, studies of the reacting flow in a packed-bed and a wall-coated reformers are carried out.

2. Experiment

2.1. Packed-bed reformer

In previous studies [17,18], experiments were carried out in a packed-bed reformer with the BASF K3-110 $CuO/ZnO/Al_2O_3$ based catalyst. Catalyst pellets were ground into powder and sieved to obtain an average diameter of 25 microns. Borosilicate

* Corresponding author. Tel.: +1 510 642 1006; fax: +1 510 642 5539.
E-mail address: mtlee@me.berkeley.edu (M.-t. Lee).

0378-7753/$ – see front matter © 2007 Elsevier B.V. All rights reserved.
doi:10.1016/j.jpowsour.2007.01.007

Nomenclature

A	1st pre-exponential coefficient [m^3 (s kg)$^{-1}$]
B	2nd pre-exponential coefficient [m^3 (s kg)$^{-1}$]
c_b	molar concentration of the stream [kmol m^{-3}] = $p/(RT)$ for ideal gas
E	activation energy [kJ $kmol^{-1}$]
F_m	methanol inlet flow rate [mol s^{-1}]
k_D	forward reaction rate constant of methanol decomposition reaction [kmol (m^3 s)$^{-1}$]
k_R	forward reaction rate constant of steam-methanol reforming reaction [l s^{-1}]
m_{cat}	mass of catalyst [kg]
M	molecular weight [kg $kmol^{-1}$]
p	pressure
$\dot{r}'''$	rate of production [kmol (m^3 s)$^{-1}$]
R	universal gas constant
SMR	steam to methanol molar ratio
T	temperature [K]
u	axial direction gas mixture velocity [m s^{-1}]
V_{in}	volumetric flow rate of methanol and water mixture at the inlet of the reformer
w'''_{cat}	density of catalyst [kg m^{-3}]
x_i	mole fraction of species i

Greek letter

ρ	density of gas mixture [kg m^{-3}]
ξ	reaction progress parameter

Subscripts

1	methanol
2	water
3	hydrogen
4	carbon dioxide
5	carbon monoxide
b	bulk value
D	value for methanol decomposition reaction
R	value for steam-methanol reforming reaction

glass tubes with 1.5 mm inner and 1.8 mm outer diameters were filled with the catalyst powder and the two ends of the packing bed were held by inserted deactivated silica wools. Fig. 1 shows a schematic of the experimental apparatus. Mixtures of distilled water and methanol with molar ratio 1.1 flowed into the evaporator at specified flow rates using a syringe pump (Genie programmable syringe pump, Kent Scientific Corp.). A k-type thermocouple was inserted in the middle of the catalyst packing bed to obtain a characteristic reformer temperature. The reactants were heated and the gas then flowed into the reformer. The reformer was heated to supply the energy for the endothermic reforming reaction. The temperature of the outer surface of the reformer was controlled by utilizing a temperature controller (Minco CT-16A). The gas leaving the reformer passed through a cold trap to separate the unreacted reactants, i.e. methanol and water. The total flow rate of the product gas mixture (H_2, CO_2 and CO) at the outlet of the cold trap was measured with a flowmeter (ADM 2000, Agilent). Tests were carried out first for a specific inlet flow rate of methanol and water mixture and the temperature was then varied for different runs [19]. The sequence was then repeated for a new inlet flow rate.

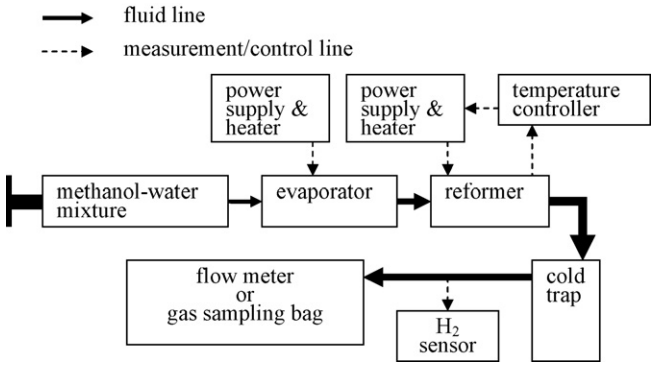

Fig. 1. Apparatus of experimental setup.

The concentration of H_2 of the product gas mixture was measured with a H_2 sensor (Robust Hydrogen Sensor, DCH Technology Inc.) and the flow rate of H_2 was then obtained by multiplying the total product gas mixture flow rate and the H_2 concentration. Assuming a small CO concentration, the flow rate of CO_2 is then obtained by subtracting the H_2 flow rate from the total flow rate.

Amphlett et al. [20] carried out experiments in a packed-bed reformer with methanol and water mixtures with the BASF K3-110 catalyst. They obtained the constants in the Arrhenius law expressions which provide the semi-empirical relations for the methanol reforming and decomposition reaction rate constants, k_R and k_D, respectively. Utilizing the reaction rate constants of Amphlett et al. [20] in conjunction with a "reaction progress variable" (cf. Appendix A), Park et al. [17,18] obtained theoretical results for the methanol conversion, the product mixture flow rate and the molar concentrations of CH_3OH, H_2O, H_2, CO_2 and CO in a packed-bed steam-methanol reformer at atmospheric pressure. Comparisons between predicted and measured H_2 and CO_2 flow rates were made and the results were in good agreement.

In the present work, another $CuO/ZnO/Al_2O_3$ based catalyst (BASF F3-01) was used in both a packed-bed and a wall-coated reformer. Tests of the catalyst were first carried out in a packed-bed reformer. Specifically, flow rates and concentrations of H_2, CO_2 and CO were measured at various reacting temperatures and flow rates of the methanol and water mixture. Particle size is an important factor for the catalyst because of intraparticle diffusion [28]. Therefore, two different catalyst particle sizes, 75 and 150 microns, were tested. 15 to 16 mg of the BASF F3-01 catalyst particles were loaded into borosilicate glass tubing having an inner/outer diameter of 1.5 mm/1.8 mm, respectively. The loading length of the catalyst was about 1.1 cm of the 75 micron catalyst particles and about 0.9 cm for the 150 micron particles. The two ends of the catalyst packing bed were sealed with silica wool. A temperature controller was used to maintain the outer surface temperature of the tubing at

Table 1
Reaction progress variable (1 = CH_3OH, 2 = H_2O, 3 = H_2, 4 = CO_2, b = bulk)

ξ	x_{1b}	x_{2b}	x_{3b}	x_{4b}	u_b	M_b
0	$\frac{1}{SMR+1}$	$\frac{SMR}{SMR+1}$	0	0	$u_{b,in}$	$\frac{18SMR+32}{SMR+1}$
$\xi(z)$	$\frac{1-\xi}{SMR+1+2\xi}$	$\frac{SMR-\xi}{SMR+1+2\xi}$	$\frac{3\xi}{SMR+1+2\xi}$	$\frac{\xi}{SMR+1+2\xi}$	$\frac{(SMR+1+2\xi)u_{b,in}}{SMR+1}$	$\frac{18SMR+32}{SMR+1+2\xi}$
1	0	$\frac{SMR-1}{SMR+3}$	$\frac{3}{SMR+3}$	$\frac{1}{SMR+3}$	$\frac{(SMR+3)u_{b,in}}{SMR+1}$	$\frac{18SMR+32}{SMR+3}$

the middle of the catalyst packing bed. Heating upstream of the reformer provided a gas phase flow of methanol/water mixtures at the inlet to the reformer. The experimental procedure was the same as described previously. The detailed operating conditions of these tests are listed in Table 2.

Deactivation of the $CuO/ZnO/Al_2O_3$ based catalyst in packed-bed reformers, especially the degradation caused by sintering, is expected even in the recommended working temperature range [29,30]. Therefore, it is essential to test the repeatability of the data before carrying out the kinetic tests. The repeatability tests for BASF F3-01 were carried out at 230 °C and a 20 μL min^{-1} inlet flow rate of a water and methanol mixture with the steam to methanol molar ratio SMR = 1.1. Fig. 2 shows the repeatability test results for the conversion which is defined as

$$\text{conversion} \equiv \frac{x_{1b,in} - x_{1b,out}}{x_{1b,in}} \times 100 \quad (1)$$

The subscript 1 refers to methanol and the subscript b refers to the bulk value. For the determination of the mole fractions $x_{1b,in}$ and $x_{1b,out}$ refer to Appendices A and B and Table 1.

The amplitude of the reduction rate of the conversion, which corresponds to the degradation rate of the catalyst activity, decreases gradually with respect to testing time for both catalyst particle sizes. This result is in agreement with the trend of deactivation of the $CuO/ZnO/Al_2O_3$ based catalyst reported previously [29,30]. After 4 h of reforming, the conversion was reduced from 43 to 38%. All other tests in this work were done within 4 h for each reformer newly loaded with catalyst. It is noted that Thurgood et al. [30] reported that the rate of decline of the catalyst activity increases with increasing reactor temperature. Results shown in this work were obtained from the experiments performed at temperatures not higher than 230 °C.

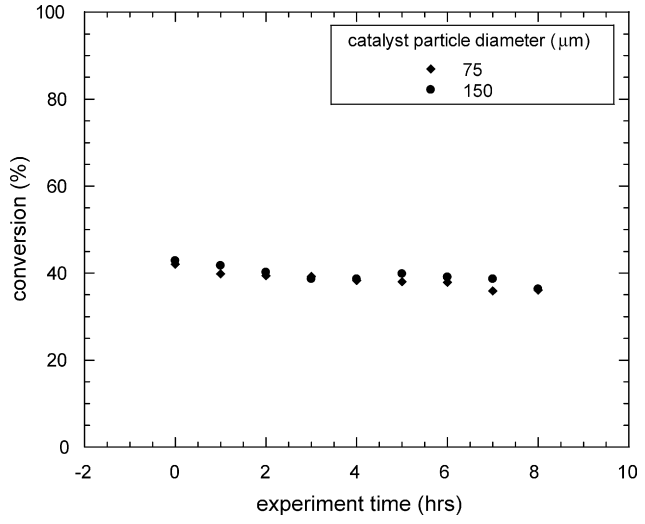

Fig. 2. Results of repeatability test for packed-bed reformers, testing at 230 °C, inlet flow rate of 20 μL min^{-1}, SMR = 1.1, catalyst loading = 16 mg.

Tests were also carried out to obtain the CO concentrations of the product gas mixtures. The experimental conditions and procedures were the same as described in the previous section. With a specified inlet flow rate of the methanol-water mixture and reformer temperature, the concentration of H_2 was measured with the DCH H_2 sensor and the product gas mixture was collected with a gas sampling bag (SKC Inc.) after the product gas mixture flow rate was stabilized. The collection of the product gas mixture for each test was completed within 3 h. The product gas mixture flow rate was checked every hour during the test to check the stability of the system. The CO concentrations in the collected gas sample bags were measured by utilizing a Fourier Transform Infrared Spectrometer (Magna 760 FTIR, Nicolet Instrument Corp.).

2.2. Wall-coated reformer

Coating of the catalytic layer was carried out following the wash-coated procedure developed by Bravo et al. [31]. Borosilicate tubes with the same size as used for the packed-bed reformer were wash-coated with the slurries made by mixing and dispersing the BASF F3-01 catalyst and distilled water. The length of the catalytic coating layer varies from 2 to 6 cm. The average coating thickness was about 100 μm. This value was obtained from the scanning electronic microscopic (SEM) images of the wash-coated reformers as shown in Fig. 3. The average loading of the catalyst was about 8 mg. Experiments and measurements were carried out with the same testing sequence as for the packed-bed reformer tests. Outer wall surface temperatures at the locations of 1/4, 1/2 and 3/4 of the coating length were monitored and maintained at the desired temperature. The operating conditions were listed in Table 2. Fig. 4 shows the result of the repeatability test of the wall-coated reformer. After 4 h of reforming, the conversion was reduced from 28% to 20%. All other tests in this study were done within 4 h for each reformer newly loaded with catalyst.

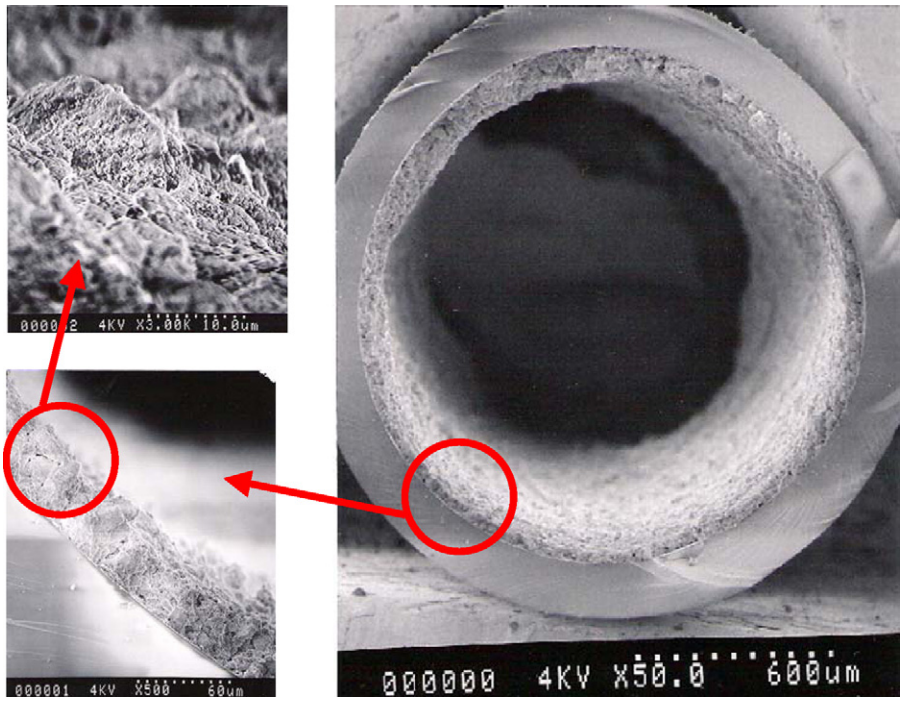

Fig. 3. Scanning electronic microscope images of wall-coated reformer. Tube i.d. = 1.5 mm. Catalyst coating thickness is about 100 μm.

Table 2
Reformer test conditions

Water to methanol molar ratio (SMR)	1.1
Feeding rate	2–30 μL min^{-1}
Reacting temperature	200–250 °C
Environment pressure	1 atm
Environment temperature	Room temperature

3. Results and discussion

3.1. Methanol conversion

Comparisons of the conversion of packed-bed and wall-coated reformers at three different reforming temperatures are shown in Fig. 5(a)–(c). The low conversion rates are mainly due to the low reactor temperatures and the small amount of catalyst loading; the methanol conversion increases with increasing reactor temperature or increasing the amount of catalyst loading (m_{cat}). It is shown that the conversion of the packed-bed reformers differs only slightly for the two different particle sizes (75 and 150 μm). Purnama et al. [28] carried out experiments on two packed-bed reformers with a CuO/ZnO/Al_2O_3 Süd-Chemie catalyst for particle sizes from 0.71 to 1.0 mm and from 0.45 to 0.5 mm, respectively, and showed that the smaller catalyst particles produced higher conversion. Jiang et al. [23] carried out methanol reforming experiments on CuO/ZnO/Al_2O_3 BASF S3-85 catalyst particles for sizes from 150 to 590 microns and noted no effect of particle size on methanol conversion. The catalyst particle sizes utilized in the present study were much smaller than were used by Purnama et al. [28] and were comparable to those used by Jiang et al. [23]. Consistent with the results of

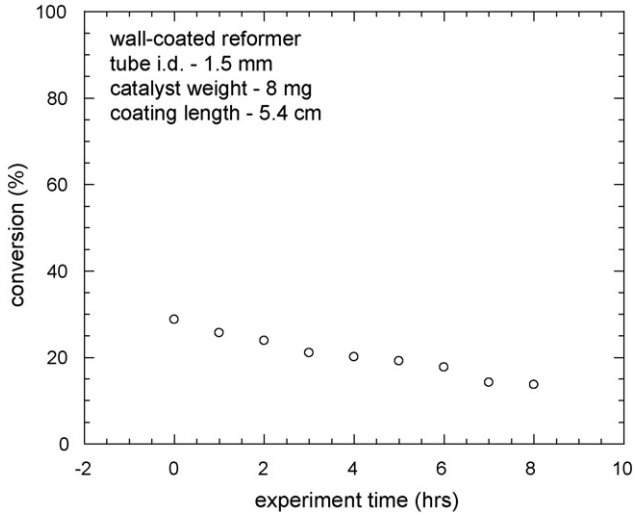

Fig. 4. Results of repeatability test for wall-coated reformer, testing at 230 °C, inlet flow rate of 20 μL min^{-1}, SMR = 1.1.

Jiang et al. [23], there was found to be little effect of the catalyst particle size on the conversion.

Bravo et al. [31] carried out methanol reforming experiments on (a) packed-bed and (b) wall-coated reformers in 4.1 mm diameter tubes that were (a) packed with 100 to 250 micron catalyst particles or (b) coated with catalyst on the inner wall surface of the tubes. They used CuO/ZnO/Al_2O_3 BASF F13456 catalyst. At the reforming temperature of 230 °C, their results showed that the wall-coated reformer produced much greater conversion than that of the packed-bed reformer. In the present study (with the catalyst BASF F3-01), the conversions produced by wall-coated reformers are very close to those of the packed-bed reformers.

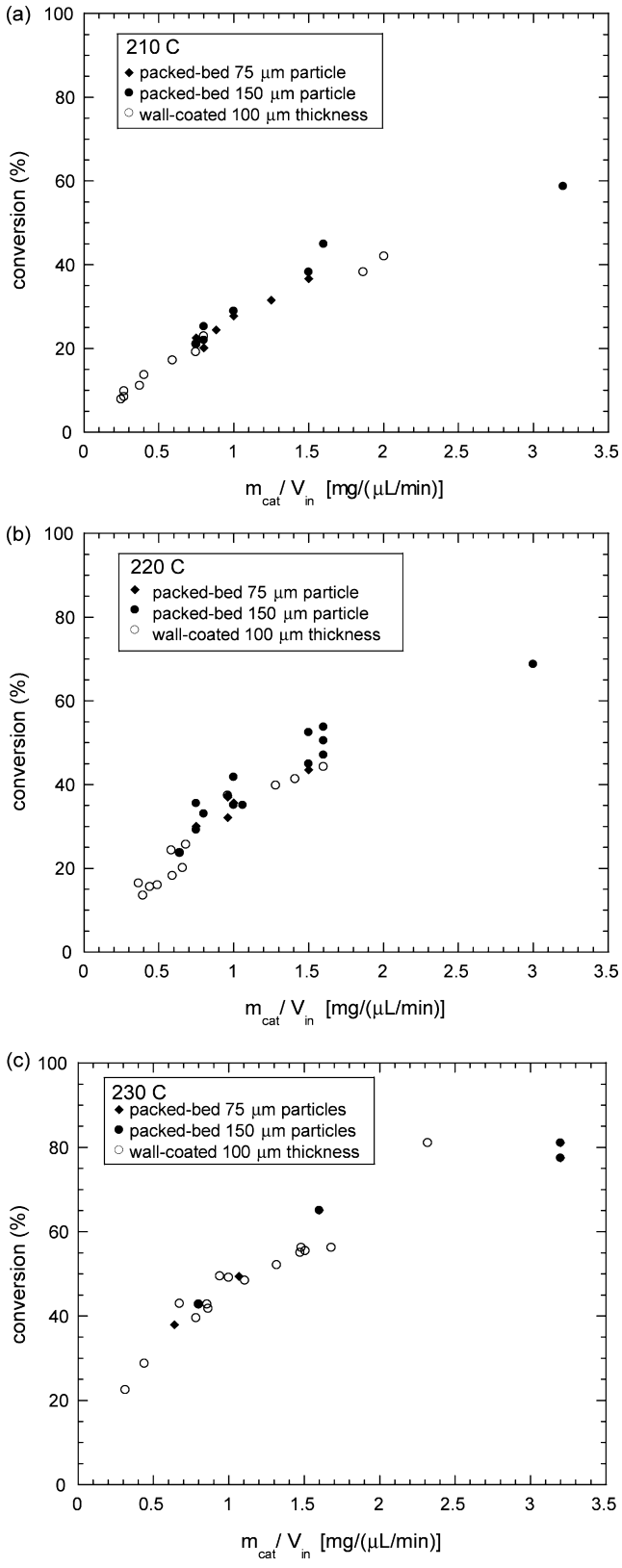

Fig. 5. Comparison of conversions of packed-bed and wall-coated reformers.

Karim et al. [16,32] carried out experiments and transport analyses on packed-bed and wall-coated reformers. Their experimental results on packed-bed reformers with tube diameters 1, 1.75 and 4.1 mm show that the conversion increased with decreasing diameter [32]. In their analysis, they noted a significant temperature difference in the packed-bed reformer with the temperature near the core being much lower than the nominal reforming temperature (which is measured at the wall surface); the reactions are endothermic and the heat was supplied to the reformer from the outside surface of the wall [16]. This results in the average temperature of the catalyst bed being significantly lower than the temperature near the wall and the temperature difference between the surface and the core of the packed-bed reformer increased with increasing tube diameter. The experimental results of wall-coated reformers with tube diameters 0.53, 1.75 and 4.1 mm obtained by Karim et al. [32] showed that the conversions are almost the same. Their analysis of the wall-coated reformer with a tube diameter of 0.53 mm showed that the temperature difference in the thin catalyst coating layer is very small so that the average temperature of the wall-coated catalyst layer is very close to the wall temperature. Additional differences between the packed-bed and wall-coated reformers should also be present corresponding to the different mass transport and surface reaction characteristics. Experimental results of Karim et al. [32] showed that at the same wall temperature the conversion produced from the packed-bed reformer with tube diameter 1 mm is greater than from the wall-coated reformers with tube diameters 0.53, 1.75 and 4.1 mm. They postulated this to result from the catalyst structure and properties that changed during the coating process.

It would appear that if the conversion is dominated by the temperature effect (distribution) then for the same wall temperature the higher average catalyst layer temperature of the wall-coated reformer should yield greater conversion than that from the packed-bed reformer. This is apparently the condition for Bravo et al. [31] but not for the present experiments which show only little difference in conversion between the packed-bed and wall-coated reformers at the same wall temperature. In the present study, a 1.5 mm diameter tube was utilized for both packed-bed and wall-coated reformers and it is expected that for the packed-bed reformer that the temperature difference in this 1.5 mm tube is less than that for the larger 4.1 mm diameter tube that was used by Bravo et al. [31]. Thus, in the present experiments the average temperatures of the packed-bed reformer and wall-coated reformer should be closer to each other than for the larger diameter tube of Bravo et al. [31] and the effect of the temperature differences, although present, should be diminished. It is noted that the experimental results obtained by Karim et al. [32] showed the conversions of packed-bed and wall-coated reformers with a tube diameter of 1.75 mm to be almost the same at the same wall temperature.

3.2. Carbon monoxide

Fig. 6 shows the results for the carbon monoxide concentration produced in the packed-bed reformers filled with 150 micron catalyst particles. The concentration of CO increases

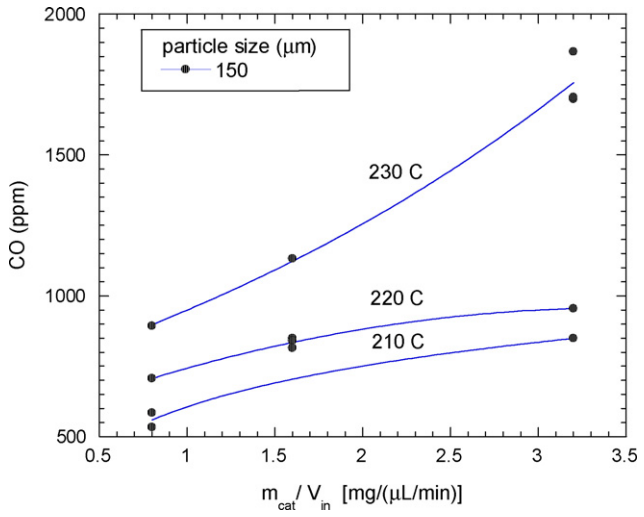

Fig. 6. Comparison of carbon monoxide concentrations produced from packed-bed reformer at various reforming temperatures.

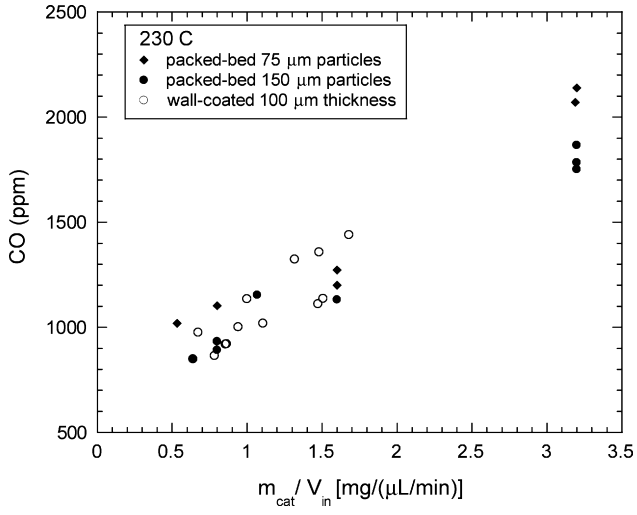

Fig. 7. Comparison of carbon monoxide concentrations produced from packed-bed and wall-coated reformers.

with respect to the value of m_{cat}/V_{in} which is proportional to the residence time or contact time that the reactants and products are in the reformer. At the same value of m_{cat}/V_{in}, the CO concentration is greater at higher temperature. Park et al. [33] measured the CO concentration produced in a micro packed-bed reformer with a specified catalyst loading weight and inlet methanol-water mixture flow rate for different reforming temperatures. They also showed an increasing concentration of CO with increased temperature. Agrell et al. [21] reported a decreasing concentration of CO with increasing steam to methanol ratio (SMR). The benefit of utilizing a greater value of SMR to minimize CO generation is offset by the lower hydrogen generation rate that results because methanol contributes more hydrogen per mole than water. Accordingly, a compromise value of SMR (1.1) was utilized in the present system.

Amphlett et al. [20] utilized the methanol decomposition reaction as the model to predict the concentration of CO and obtained a result for the CO concentration that is linearly dependent on the residence time. Recent studies [21,27,34] have suggested that in steam-methanol reforming with the $CuO/ZnO/Al_2O_3$ based catalyst, CO is produced as a secondary product from the reverse water-gas-shift reaction (Eq. (2))

$$CO_2 + H_2 \rightarrow CO + H_2O \quad (2)$$

rather than from methanol decomposition.

Based on their experimental results, Purnama et al. [28] further suggested that the controlling kinetics of CO formation is dependent on the magnitude of the residence time and reforming temperature. The experimental results of CO concentration obtained in the present study are consistent with the trend presented in the study by Purnama et al. [28].

Fig. 7 shows a comparison of the CO concentration produced from two packed-bed (filled with catalyst particles of diameters 150 microns and 75 microns) and wall-coated reformers at the reforming temperature of 230 °C. It is shown that the CO concentrations produced from all the tests are similar to each other at the same value of m_{cat}/V_{in}.

Bravo et al. [31] carried out similar tests in a wall-coated reformer with a 25 micron thick catalyst layer wash-coated on the inner wall of a 4.1 mm inner diameter glass tube. They also carried out tests in a packed-bed reformer with a 4.1 mm i.d. glass tube filled with 100–250 micron catalyst particles. The CO concentration was higher for the wall-coated reformer than for the packed-bed reformer at the same value of the catalyst weight to methanol inlet flow rate ratio (m_{cat}/F_m). It is noted that Bravo et al. [31] presented their CO results with respect to the conversion. Using this result, and their conversion results with respect to m_{cat}/F_m, we obtained the result noted above for CO concentrations with respect to m_{cat}/F_m. It is also pointed out that Bravo et al. [31] showed that the CO concentration is less for the wall-coated reformer than for the packed-bed reformer at the same value of the conversion. These differences of CO concentrations between the packed-bed and wall-coated reformers were attributed to result mainly from the temperature variation across the reformer as described in the previous section.

In the present study, however, the differences of the CO concentrations for the two reformers are not as large as were observed by Bravo et al. [31]. We have pointed out that the tube being used as the reformer in the present study is smaller than that used by Bravo et al. [31]. The temperature difference across the catalyst bed in the packed-bed reformer should be smaller in the smaller tube. Thus, the average temperatures of the packed-bed and wall-coated reformers are closer to one another and the effect of the temperature differences is diminished in the present study.

4. Conclusions

Packed-bed and wall-coated methanol-steam reformers were studied in the present work. The results show that the methanol conversion was reduced by 5–8% after 4 h of continuous reforming and the amplitude of the reduction rate decreased gradually with testing time. Under the same reforming condition, the packed-bed reformer filled with 150 micron or with 75 micron catalyst

particles produced the same methanol conversion and CO concentration. At the same reformer wall temperature, the methanol conversion and CO concentration produced from the packed-bed reformer and from the wall-coated reformer are the same for the same value of the catalyst mass to inlet fuel flow rate ratio (m_{cat}/V_{in}). This result indicates that at the same wall temperature that the average temperature of the catalyst bed in the packed-bed reformer is close to the average temperature of the catalyst layer in the wall-coated reformer.

Acknowledgment

The BASF F3-01 catalyst was provided by BASF Inc. We thank Dr. Jeffrey D. Morse of Lawrence Livermore National Laboratory (LLNL) who provided technical supports on the reformer studies and Dr. Donald Lucas of Lawrence Berkeley National Laboratory (LBNL) who provided technical and experimental support for the carbon monoxide measurements. We also thank Stephen Sharratt and Allan Chen who assisted in carrying out the measurements. This work was partially supported by the Industrial Technology and Research Institute (ITRI) in Taiwan, R.O.C. and the Berkeley ITRI Research Center (BIRC).

Appendix A. Reaction progress variable (Park et al. [17,18])

The kinetics of steam-methanol reforming reaction has been studied intensively; a number of kinetic models have been proposed [20–27], and the model of Amphlett et al. [20] is utilized. In Amphlett's analysis, the steam-methanol reforming reaction can be modeled with two major reactions:

$$\text{Reforming reaction} \quad CH_3OH + H_2O \underset{k_{R'}}{\overset{k_R}{\leftrightarrow}} 3H_2 + CO_2 \tag{A1}$$

$$\text{Decomposition reaction} \quad CH_3OH \cdot \xrightarrow{k_D} 2H_2 + CO \tag{A2}$$

The water-gas shift reaction was assumed in Amphlett's analysis to have negligible impact. Reaction rates of the reforming and decomposition reactions can be expressed as follows:

$$\dot{r}_R''' = k_R c_{1b} \tag{A3}$$

$$k_R = w_{cat}'''[A_R + B_R \ln(\text{SMR})] \exp\left[-\frac{E_R}{\bar{R}T}\right] \tag{A4}$$

$$\dot{r}_D''' = k_D \tag{A5}$$

$$k_D = w_{cat}''' A_D \exp\left[-\frac{E_D}{\bar{R}T}\right] \tag{A6}$$

The reaction rate of the reforming reaction is found to be much greater than the decomposition rate due to the selectivity of the catalyst and is thus the main source of hydrogen generation. To obtain the amount of carbon monoxide generation, Amphlett used the decomposition reaction and is utilized in this study.

If initially there is one mole methanol and SMR moles of water vapor, the molar fractions of methanol and water vapor can be expressed as $x_{1b} = 1/(1 + \text{SMR})$ and $x_{2b} = \text{SMR}/(1 + \text{SMR})$, respectively. There is no hydrogen or carbon dioxide at the entrance to the reformer.

As reaction occurs on the catalyst as reactants flow toward the downstream of the reformer, hydrogen is generated as the main product and carbon dioxide is produced as the main byproduct. Presuming ξ, moles of methanol having been reacted after some distance z from the reformer entry, referring to the steam-methanol reforming reaction (A1), ξ, moles of water vapor have also been reacted and 3ξ, moles of hydrogen as well as ξ, moles of carbon dioxide have been generated. The molar ratio of each of the four major species can then be obtained as a function of ξ, and is listed in Table 1. The value of ξ, increases as the reforming reaction continues. With methanol being completely reformed, there will be 3 moles of H_2 and 1 mole of CO_2 as products; SMR-1 moles of water and no methanol are left as reactants, as listed in Table 1.

With knowing the molar fractions of the four major species, the molecular weight, M_b, of the reacting gases flow as function of ξ, can therefore be obtained. Also, by assuming ideal gas, isothermal and constant pressure, the expressions for average velocity, u_b can be derived, as summarized in Table 1.

The bulk density, ρ_b, can also be obtained from the ideal gas law:

$$\rho_b = M_b \left(\frac{p_b}{RT_b}\right) = M_b c_b \tag{A7}$$

Appendix B. Procedure for evaluating mole fractions

Refering to Appendix A and Table 1 the mole fraction x_{1b} is given by

$$x_{1b} = \frac{1 - \xi}{\text{SMR} + 1 + 2\xi} = \frac{1 - \xi}{2.1 + 2\xi} \tag{B1}$$

where SMR = 1.1. To obtain $x_{1b,out}$, the value of ξ_{out} is obtained from Table 1 for $u_b = u_{b,out}$:(B2)$u_{b,out} = \frac{(2.1+2\xi_{out})u_{b,in}}{2.1}$The measured values of $u_{b,in}$ and $u_{b,out}$ then yield the value of ξ_{out} which then yields $x_{1b,out}$ from Eq. (B1).

$$\text{Note that} \quad x_{1b,in} = \frac{1}{2.1} \tag{B3}$$

References

[1] F. Barbir, PEM Fuel Cells: Theory and Practice, Elsevier Academic Press, MA, USA, 2005.
[2] H.L. Maynard, J.P. Meyers, J. Vac. Sci. Technol. B 20 (4) (2002).
[3] J.B. Hansen, Handbook of Fuel Cells – Fundamentals, Technology and Applications, vol. 3, John Wiley & Sons, Ltd., New York, 2003, pp. 141–148.
[4] K.F. Jensen, Chem. Eng. Sci. 56 (2001) 293–303.
[5] B. Lindstrom, J. Agrell, L.J. Pettersson, Chem. Eng. J. 83 (2003) 91–101.
[6] S. Tanaka, K.S. Chang, K.B. Min, D. Satoh, K. Yoshida, M. Esashi, Chem. Eng. J. 101 (2004) 143–149.
[7] G.G. Park, D.J. Seo, S.H. Park, Y.G. Yoon, C.S. Kim, W.L. Yoon, Chem. Eng. J. 101 (2004) 87–92.
[8] O.J. Kwon, S.M. Hwang, J.G. Ahn, J.J. Kim, J. Power Sources 156 (2006) 253–259.
[9] K.S. Chang, S. Tanaka, M. Esashi, J. Micromech. Microeng. 15 (2005) S171–S178.

[10] T. Terazaki, M. Nomura, K. Takeyama, O. Nakamura, T. Yamamoto, J. Power Sources 145 (2005) 691–696.
[11] Y. Kawamura, N. Ogura, T. Yamamoto, A. Igarashi, Chem. Eng. Sci. 61 (2006) 1092–1101.
[12] J.D. Holladay, E.O. Jones, M. Phelps, J. Hu, J. Power Sources 108 (2002) 21–27.
[13] J.D. Holladay, E.O. Jones, R.A. Dagle, G.G. Xia, C. Cao, Y. Wang, J. Power Sources 131 (2004) 69–72.
[14] J. Morse, A. Jankowski, US Patent No. US690235 (2005).
[15] S. Nagano, H. Miyagawa, O. Azegami, K. Ohsawa, Energy Convers. Manage. 42 (2001) 1817–1829.
[16] A. Karim, J. Bravo, A. Datye, Appl. Catal. A: Gen. 282 (2005) 101–109.
[17] H.G. Park, J. Chung, C.P. Grigoropoulos, R. Greif, M. Havstad, J.D. Morse, Proceedings of 2003 ASME Summer Heat Transfer Conference, Las Vegas, Nevada, USA, HT2003-47216, July 21–23, 2003.
[18] H.G Park, M.T. Lee, F.K. Hsu, C.P. Grigoropoulos, R. Greif, C.H. Lin, Proceedings of IMECE 2004, Anaheim, CA, USA, JMECE2004-61208, November 13–19, 2004.
[19] S.P. Asprey, B.W. Wojciechowski, B.A. Peppley, Appl. Catal. A: Gen. 179 (1999) 51–70.
[20] J.C. Amphlett, K.A.M. Davis, R.F. Mann, B.A. Peppley, D.M. Stokes, Int. J. Hydrogen Energy 19 (2) (1994) 131–137.
[21] J. Agrell, H. Birgersson, M. Boutonnet, J. Power Sources 106 (2002) 249–257.
[22] C.J. Jiang, D.L. Trimm, M.S. Wainwright, Appl. Catal. A: Gen. 97 (1993) 145–158.
[23] C.J. Jiang, D.L. Trimm, M.S. Wainwright, Appl. Catal. A: Gen. 93 (1993) 245–255.
[24] B.A. Peppley, J.C. Amphlett, L.M. Mearns, L.F. Mann, Appl. Catal. A: Gen. 179 (1999) 21–29.
[25] B.A. Peppley, J.C. Amphlett, L.M. Mearns, R.F. Mann, Appl. Catal. A: Gen. 179 (1999) 31–34.
[26] Y. Choi, H.G. Stenger, J. Power Sources 142 (2005) 81–91.
[27] J.K. Lee, J.B. Ko, D.H. Kim, Appl. Catal. A: Gen. 278 (2004) 25–35.
[28] H. Purnama, T. Ressler, R.E. Jentoft, H. Soerijanto, R. Schlogl, R. Schomacker, Appl. Catal. A: Gen. 259 (2004) 83–94.
[29] D.G. Loffler, S.D. McDermott, C.N. Renn, J. Power Sources 114 (2003) 15–20.
[30] C.P. Thurgood, J.C. Amphlett, R.F. Mann, B.A. Peppley, Topics Catal. 22 (3–4) (2003).
[31] J. Bravo, A. Karim, T. Conant, G.P. Lopez, A. Datye, Chem. Eng. J. 101 (2004) 113–121.
[32] A. Karim, J. Bravo, D. Gorm, T. Conant, A. Datye, Catal. Today 110 (2005) 86–91.
[33] H.G. Park, J.A. Malen, W.T. Piggott, III, J.D. Morse, R. Greif, C.P. Grigoropoulos, M.A. Havstad, R. Upadhye, J. MEMS 15 (4) (2006).
[34] J.P. Breen, J.R.H. Ross, Catal. Today 51 (1999) 521.